Low-altitude signatures of the cusp and flux transfer events

Article

Published Version

GEOPHYSICAL RESEARCH LETTERS, VOL. 16, NO. 8, PAGES 879-882, AUGUST 1989

LOW-ALTITUDE SIGNATURES OF THE CUSP AND FLUX TRANSFER EVENTS

Mike Lockwood

Rutherford Appleton Laboratory, Chilton, UK

Mark F. Smith

Southwest Research Institute, San Antonio, USA

Abstract The usual interpretation of a flux transfer event (FTE) at the magnetopause, in terms of time-dependent and possibly patchy reconnection, demands that it generate an ionospheric signature. Recent ground-based observations have revealed that auroral transients in the cusp/cleft region have all the characteristics required of FTE effects. However, signatures in the major available dataset, namely that from low-altitude polar-orbiting satellites, have not yet been identified. In this paper, we consider a cusp pass of the DE-2 spacecraft during strongly southward IMF. The particle detectors show magnetosheath ion injection signatures. However, the satellite motion and convection are opposed, and we discuss how the observed falling energy dispersion of the precipitating ions can have arisen from a static, moving or growing source. The spatial scale of the source is typical of an FTE. A simple model of the ionospheric signature of an FTE reproduces the observed electric and magnetic field perturbations. Precipitating electrons of peak energy ~100eV are found to lie on the predicted boundary of the newly-opened tube, very similar to those found on the edges of FTEs at the magnetopause. The injected ions are within this boundary and their dispersion is consistent with its growth as reconnection proceeds. The reconnection potential and the potential of the induced ionospheric motion are found to be the same (≈25kV). The scanning imager on DE-1 shows a localised transient auroral feature around DE-2 at this time, similar to the recent optical/radar observations of FTEs.

Introduction

The cusp is a region where magnetosheath plasma is injected into the magnetosphere and ionosphere. The restricted extent of this source and the convection electric field cause energy dispersion of ions observed in the ionosphere (see discussion by Smith et al. 1989). A Flux Transfer Event (FTE) is a signature in the magnetic field seen near the magnetopause, interpreted as resulting from time-dependent reconnection (Russell and Elphic, 1978). Inside an FTE there is a layered mixing of magnetosphere and magnetosheath plasma. Recently Menietti and Burch (1988) have shown cusp injections have a similar spatial extent as FTEs and suggested the two phenomena may be linked.

Observations by ground-based optical photometers and T.V. all-sky cameras have revealed transient, short-lived arcs (in both 630nm and 557.7nm emissions) occurring throughout the dayside auroral oval when the IMF is southward, superposed on the persistent "cleft" aurora (630nm only). Recently, Lockwood et al. (1989) have shown that each optical event is accompanied by a transient flow burst of ionospheric plasma, and that considerable potentials (20-55 kV) were applied across the field-of-view of the EISCAT radar. Sandholt et al. (1989) have studied a pass of the HILAT satellite through one of these events and found particle injection signatures and filamentary field-aligned currents. These transient events have been shown to be fully consistent with magnetopause FTEs: in their occurrence (during southward IMF only); motion (west or east, depending on IMF B_y, before turning into the polar cap); field-aligned currents (oppositely directed matched pair); ionospheric flow (twin vortical); scale size (few hundred kilometres); and potentials. In this paper, we study cusp-like ion injection using a pass of the DE-2 satellite. In the light of the above observations, we consider the injection in terms of an FTE.

Paper number 89GL01352.
0094-8276/89/89GL-01352$03.00

DE-2 Observations

Figure 1 shows data from a northern hemisphere pass of DE-2 on 22 October, 1981 at a height of 900 km. Data are shown from the Low-Altitude Plasma Instrument (LAPI), Ion Drift Meter (IDM) and the magnetometer (MAG-B). For more details of these and DE-1 data see Smith et al. (1989). The IMF was observed by ISEE-3 to turn southward at about 08 UT on this day following a 10-hour period when it was northward. Allowing for the predicted propagation delay, the near-Earth IMF was strongly southward (B_z≈-10nT) at the time of this event. The B_y component was large and positive (≈+10nT).

Panel (a) shows the fluxes of electrons of energy greater than 35keV at pitch angles of 0° (in blue) and 90° (in red). The anisotropic fluxes (showing a loss cone in the pitch angle distribution) observed before 09:55:20UT define the flux tubes as being closed: subsequently the lower, isotropic fluxes indicate open field lines. Panels (b) and (c) are energy-time spectrograms of precipitating ions and electrons, respectively.

The ion data appear to show the classic cusp ion injection signature with lower energy ions observed as the satellite moves poleward. However, panel (e) shows that the RAM component of the drift, V_r, is positive when the ions are observed (09:55:30-09:55:48), i.e. in the opposite direction to the satellite motion. For this case, a steady-state two dimensional time-of-flight model predicts ion energy rising with time, the opposite to what is observed. Hence we must consider the third spatial dimension and/or temporal variations. The satellite path is northeastward, and the cross and ram drifts (panels d

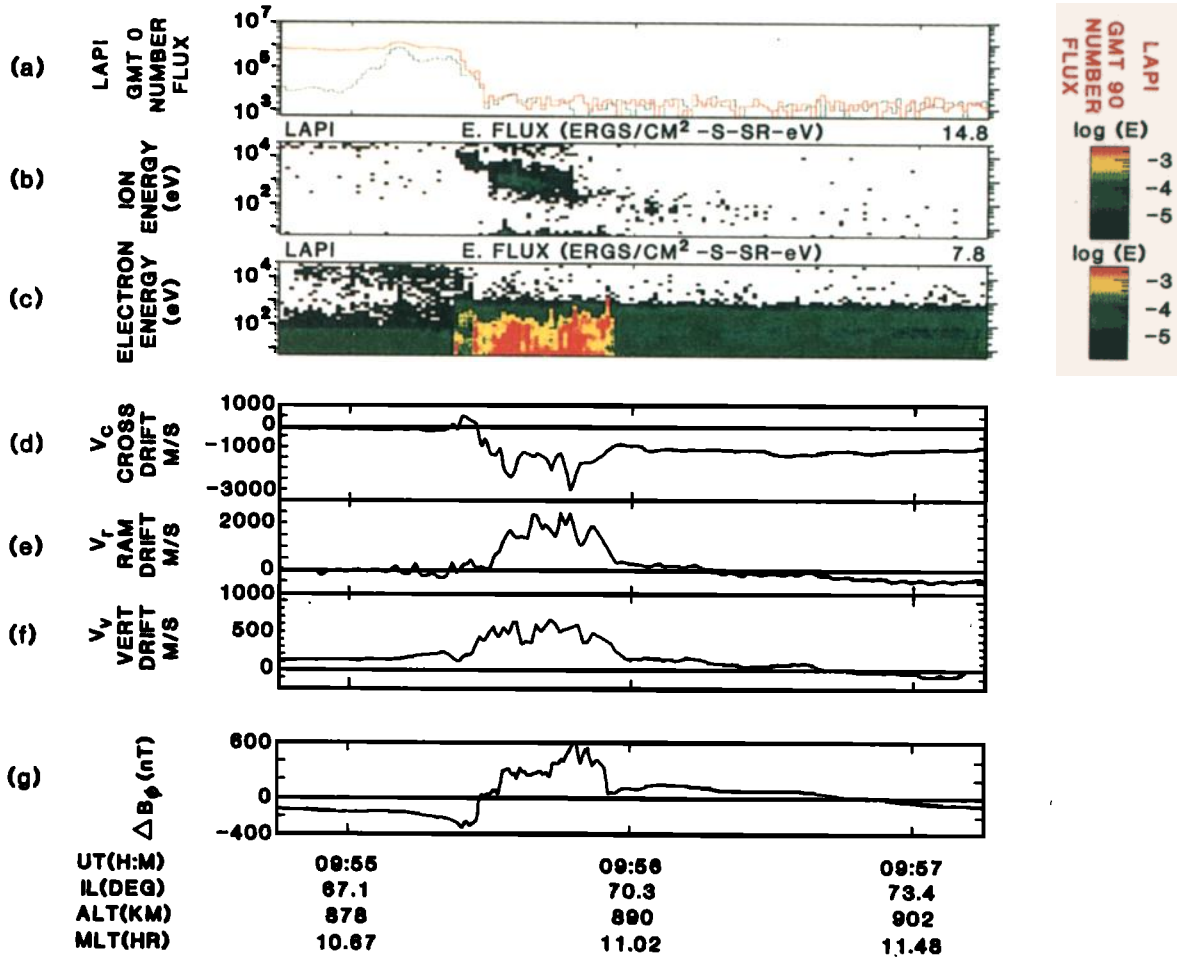

Fig. 1. Data from DE-2 on 22 October, 1981.

and e of fig. 1) give plasma flow just south of westward when the injected ions are seen. This motion is found to be aligned with the morning-sector polar cap boundary, as defined by the DE-1 imager (discussed later) , and is consistent with reconnection for the observed IMF $B_y > 0$. Panels (f) and (g) show that large upward flows of ionospheric ions and intense field-aligned currents (the latter seen by their effect on the eastward component of the magnetic field, ΔB_ϕ) are also present near the injected ions.

Hodograms of the field-perpendicular disturbance of the magnetic field observed by MAG-B reveal that the field rotated first from south-westward to south-eastward via southward. Subsequently, a weaker perturbation was superposed with a rotation in the opposite sense from north-eastward to north-westward (Smith et al., 1989). These rotations occur during the two major changes in ΔB_ϕ shown in Figure 1(g) and show that the satellite passed to the east of a pair of filamentary field-aligned currents, the upward current being roughly 150 km poleward of the downward one. If these two form a matched pair, the satellite must have passed considerably closer to the downward current, as the magnetic perturbation it caused was greater.

Simple Model of FTE Effects

We employ the model of FTE field perturbations in the ionosphere by Southwood (1987), in which momentum is transferred to the ionosphere by a pair of oppositely-directed field-aligned currents on the flanks of the newly-opened flux tube. Part (a) of figure 2 shows the ionospheric footprint of a circular tube. Also shown is a snapshot of the ionospheric flow equipotentials, in the frame fixed with respect to the Earth. If it is assumed that the satellite intersects the open tube (as is required if the ion injection is indeed due to an FTE) between 09:55:30 and 09:55:48, the mean cross and ram drifts for this period do not show any consistent rotational flow (twisting). This being the case, the Southwood FTE model applies, for which the velocity at all points within the event is that of the event itself. The means of V_c and V_r define this event velocity to be 2.5 km s^{-1}, in a direction at 138° to the satellite orbit. The straight line in the figure shows a satellite locus, relative to the open flux tube, for this event velocity and the satellite velocity of 7.4 km s^{-1}. The vectors $\overline{V}_c$ and $\overline{V}_r$ show the directions of the measured cross and ram drifts.

With the above assumptions, the model of the event intersection is uniquely determined by one variable, the distance of closest approach of the satellite to the event centre. This has been chosen to make the satellite intersect the open tube yet pass to the east of both current filaments. The variations of V_c and V_r shown in figure 2 have many of the features of the observations. It is noticable that the effect on closed field lines is much smaller than predicted and a cross drift persists on open field lines after the event. These differences can be quantitatively explained by generalising the shape of the event from a circle, by considering the event as growing in size at it propagates, or by superposing the event on a background flow.

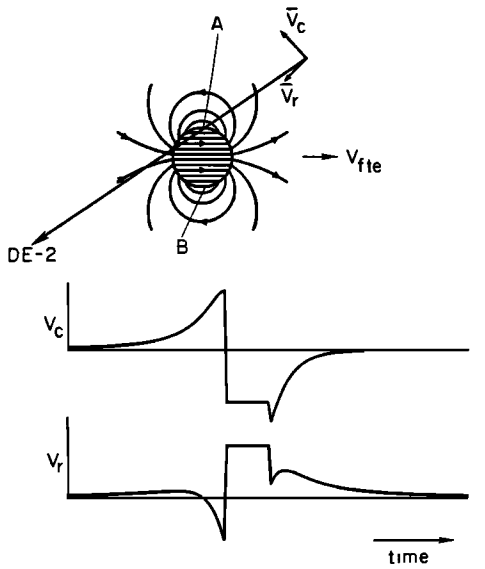

Fig. 2. Model flow components $\overline{V}_c$ and $\overline{V}_r$ as a function of time for an intersection of a circular open flux tube (velocity $\overline{V}_p$ = 2.5 km s^{-1}) and DE-2 (velocity 7.4 km s^{-1} at 138° to $\overline{V}_p$) shown at top of figure, which also gives a snapshot of induced flow equipotentials.

The boundaries of the event defined by this model place the injected ions within the newly-opened flux tube and the bursts of precipitating electrons [fig. 1 (c)] on the boundaries. These are similar to the streaming electrons found on the edges of FTE open flux tubes at the magnetopause and are explained in the FTE models by Southwood et al. (1988) and Scholer (1988) as arising from continuing, slower reconnection. An 18-second intersection with the open flux tube gives an event diameter of 170 km for this model circular tube and the path shown in Figure 2. Integrating the observed electric field across this diameter yields a potential of 25.5 kV. The above discussion provides just one of a number of possible interpretations of the flow data in terms of an FTE. In the next section we discuss how other data, particularly that from the magnetometer, are also consistent with the intersection described in Figure 2.

Discussion of FTE Model

From the particle data, we estimate the height-integrated Pedersen conductivity in the injection event to be 10 mhos, giving total field-aligned currents of 2.5 x 10^5 A for the electric field inside the event observed by IDM. The peak magnetic perturbations observed place the downward and upward currents 33 and 100 km, respectively, to the west of DE-2 at the times of observation. Using the direction of event motion derived from the IDM data, a simple geometric construction shows the current filaments to be 170 km apart and to be moving at 2.3 km s^{-1}. These values are very similar to those derived in the previous section. Hence the IDM and MAG-B data are consistent with the Southwood (1987) model of the ionospheric signature of an FTE, with an oppositely-directed pair of field-aligned currents on the flanks of a moving, newly-opened flux tube.

The events described by Lockwood et al. (1989) were observed under very similar IMF conditions and were first observed on the equatorward boundary of the persistent cleft aurora (moving rapidly westward) and faded 1-2° poleward of it after a lifetime of up to 15 min. Evidence that the event described here is accompanied by a similar auroral event comes from the scanning global imager on DE-1. Figure 3 shows the geographic latitude of peak auroral emissions at three geographic longitudes as a function of time. DE-2 intersected the event near geographic co-ordinates (68°, 341°). The scans show a general equatorward motion of the oval, consistent with an expanding polar cap following the southward turning of the IMF. Superposed on this general trend is a slight equatorward motion seen at longitudes 0° and 30° (i.e. east of DE-2) at some time between 09:45 and 09:55, followed by a poleward motion between 09:55 and 10:05. The event does not appear to reach longitude 330°. Hence the imager data are consistent with a transient event occuring around DE-2, at the time of the ion injection event, similar to those recently reported from the ground.

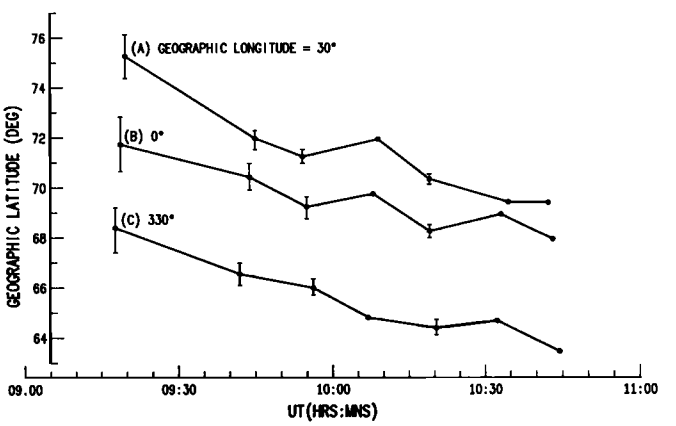

Fig. 3. Latitudes of peak auroral emissions as a function of time at 3 longitudes, from the scanning imager on DE-1 on 22 October 1981.

Discussion of Ion Injection

Figure 4 shows schematically three ways in which the observed ion dispersion could have arisen. In all three cases, the ionospheric projection of the injection region required is shown (roughly to scale) relative to the path of DE-2, which observed injected ions between points A and B. Figure 4(a) shows how the dispersion can arise from a static source, of dimensions roughly 3 R_E by 0.5 R_E, angled at 30° to the convection velocity vector, $\overline{V}_p$. These dimensions are calculated from the ions' time of flight by using a simple model of the magnetic field with the magnetopause at 10 R_E. Spatial variations in $\overline{V}_p$ between a static source and DE-2 can be invoked to give a similar result. The second possibility, b, is of a region 0.5 R_E long, perpendicular to $\overline{V}_p$, moving towards DE-2. To give the falling ion energies observed, the injection region at the magnetopause must be approaching the satellite at a speed exceeding the local convection speed.

In this paper, we do not wish to discuss the likelihood of the flow geometry and source motion

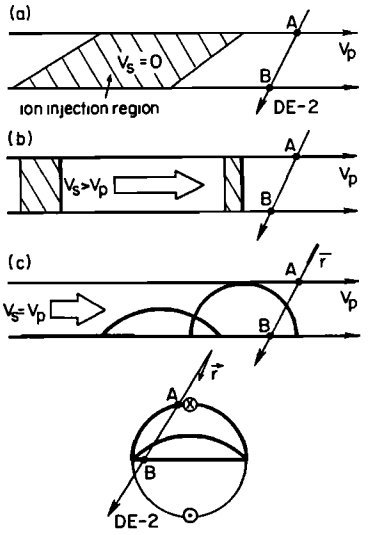

Fig. 4. Schematic of three models of ion injection giving falling ion energies at DE-2 between A and B: V_s is the velocity of the ionospheric projection of the source region, $\overline{V}_p$ is the ionospheric convection velocity.

required by these static and moving source models, respectively. Rather, we wish to point out that the particle data are consistent with a third model: that of a growing source region. This model, unlike the two mentioned above, offers an explanation of the drifts, field-aligned currents and auroral motions observed. Figure 4(c) shows how the observed dispersion could arise from a motion of the injection region perpendicular to $\overline{V}_p$. In effect, DE-2 sees more recently injected ions first (higher energies at A) as the injection region is propagating equatorward while the satellite moves poleward. We imagine the injection to occur on the leading edge of a region of newly-opened flux as it expands, due to a burst of reconnection. The lowest part of figure 4 shows the same evolution of the injection line and newly-opened flux regions, this time in the frame moving with the open flux tube. Allowing for times of flight, the lowest energy (i.e earliest injected) ions seen by DE-2 between points A and B show the growth occurred over 67 seconds - a reasonable reconnection time for an FTE. Assuming the flux tube is circular after this growth, a total of 1.53×10^6 Wb has been added, giving a reconnection potential of 23 kV. This is strikingly similar to the potential of 25 kV previously found to be associated with the motion of the event. To give the observed highest energy ions, the injection must last for 200 seconds. This figure is found to be roughly the same for all points between A and B, and in this model, is the time to empty the newly-opened tube of mixed magnetosphere and magnetosheath ions. Note that precipitating ions of energies above about 10 keV can be seen in figure 1(b) until 09:55:50, i.e. on closed and on what we suggest here are the newly-opened flux tubes of an FTE. None are seen on the open field lines after 09:55:48. It is, at first sight, surprising that ions, presumably of magneto-spheric origin, continue to precipitate after reconnection. However, the magnetic "bottle" which can trap such ions around the minimum in the magnetic field at middle latitudes of cusp field lines will not be lost until the field line is straightened. Hence ions scattered from large pitch angles will precipitate until the equatorial magnetic mirror ceases to be effective. The combination of energetic electron isotropy and 10 keV precipitating ions indicates the injection region is indeed a newly-reconnected flux tube.

Conclusions

The ion dispersion, precipitating electrons and electric and magnetic field perturbations observed by DE-2 during a dayside auroral pass are shown to be consistent with, and well explained by, a model of the reconnection and motion of an FTE flux tube. The potentials associated with the growth and motion of the event are found to be the same, as required by the Southwood FTE model. We note that consideration of the particle data from the region inside the newly-opened flux tube alone, the ion injection would have been termed the "cusp" and could be explained in terms of steady-state convection and particle injection, provided a three-dimensional model is used. However, this does not explain the filamentary field-aligned currents, the electron precipitation structure and the transient auroral motions observed during this event, which strongly suggest temporal variations in both convection and injection.

Acknowledgements. The authors are grateful to J. D. Winningham, R.A. Heelis, J.A. Slavin and J.D. Craven for provision of data and discussions of the work, for which we also thank D.J. Southwood, S.W.H. Cowley and M.P. Freeman. This research is supported by NASA grant NAGW-1638.

References

Lockwood, M., P.E. Sandholt and S.W.H. Cowley, Dayside auroral activity and magnetic flux transfer from the solar wind, Geophys Res. Lett, 16, 33, 1989.

Menietti, J.D., and J.L. Burch, Spatial Extent of the Plasma Injection Region in the Cusp-Magnetosheath Interface, J. Geophys. Res., 93, 105, 1988.

Russell, C.T. and R.C. Elphic, Inital ISEE magnetometer results: magnetopause observations, Space Sci. Rev., 22, 681, 1978.

Sandholt, P.E., et al., Electro-dynamics of the polar cusp ionosphere - A case study, J. Geophys. Res., in press, 1989.

Scholer, M. Magnetic flux transfer at the magnetopause based on single X-line bursty reconnection Geophys. Res. Lett., 15,291, 1988.

Smith, M.F., et al., Spacecraft Observations of Plasma Injections and Associated Phenomena near the cusp, J. Geophys. Res., submitted, 1989.

Southwood, D.J. The ionospheric signature of flux transfer events, J.Geophys. Res.,92,3207, 1987.

Southwood, D.J., C.J. Farrugia and M.A. Saunders, What are flux transfer events?, Planet. Space Sci., 36, 503, 1988.

M. Lockwood, Rutherford Appleton Laboratory, Chilton, Didcot, Oxon., OX11 OQX, U.K.

M.F. Smith, Southwest Research Institute, P.O Drawer 28510, San Antonio, Texas 78284, U.S.A.

(Received: 13 April 1989;
revised: 16 May 1989;
accepted: 9 July 1989)